AEM
Journals.ASM.org

Dimethyl Sulfoxide and Ethanol Elicit Increased Amyloid Biogenesis and Amyloid-Integrated Biofilm Formation in *Escherichia coli*

Ji Youn Lim, Janine M. May, and Lynette Cegelski

Department of Chemistry, Stanford University, Stanford, California, USA

***Escherichia coli* directs the assembly of functional amyloid fibers termed "curli" that mediate adhesion and biofilm formation. We discovered that *E. coli* exhibits a tunable and selective increase in curli protein expression and fiber assembly in response to moderate concentrations of dimethyl sulfoxide (DMSO) and ethanol. Furthermore, the molecular alterations resulted in dramatic functional phenotypes associated with community behavior, including (i) cellular agglutination in broth, (ii) altered colony morphology, and (iii) increased biofilm formation. Solid-state nuclear magnetic resonance (NMR) spectra of intact pellicles formed in the presence of [$^{13}C_2$]DMSO confirmed that DMSO was not being transformed and utilized directly for metabolism. Collectively, the chemically induced phenotypes emphasize the plasticity of *E. coli*'s response to environmental stimuli to enhance amyloid production and amyloid-integrated biofilm formation. The data also support our developing model of the extracellular matrix as an organized assembly of polymeric components, including amyloid fibers, in which composition relates to bacterial physiology and community function.**

Escherichia coli directs the assembly of functional amyloid fibers (termed "curli") at the bacterial cell surface. Since the discovery of curli as adhesive fimbriae in 1989 (58) and the identification of curli as amyloid in 2002 (15), we now appreciate that functional amyloids are prevalent among microorganisms, e.g., *Salmonella* and *Pseudomonas* species, *Streptomyces coelicolor*, *Mycobacterium tuberculosis*, and *Bacillus subtilis* (1, 4, 11, 15, 21, 58, 64). The assembly of functional amyloids in microbes is regulated in order to direct polymerization at the right time and place and to prevent toxicity (4, 24). In this way, the formation of functional amyloids is juxtaposed to the undesired protein misassembly events and assembly of amyloidogenic protein oligomers and amyloid fibers associated with human diseases such as Alzheimer's disease (27). The assembly of curli in *E. coli* requires the expression and proper interactions of several proteins encoded by the divergently transcribed *csgBA* and *csgDEFG* operons (*csg* [for curli-specific genes]) (16, 66). *In vivo* polymerization of the major curli subunit, CsgA, into β-sheet-rich amyloid fibers depends on the nucleating activity of the minor subunit, CsgB (38). CsgE, CsgF, and CsgG are assembly factors required for the stabilization of CsgA and CsgB and their transport to the cell surface (57, 63).

Curli are among the most well-studied microbial amyloids and have been ascribed roles in environmental persistence and transmission due to their ability to mediate adhesion to abiotic surfaces, such as stainless steel, and to biotic surfaces, including plant leaves (3, 4, 8, 67). Adhesion to both abiotic and biotic substrates can contribute to food-borne outbreaks by pathogenic strains such as *E. coli* O157:H7 (60, 78, 80). Curli also promote cellular aggregation and serve as an adhesive scaffold to promote community behavior and biofilm assembly (45, 77, 83). Biofilms are multicellular communities characterized by a complex extracellular matrix and contribute to persistence in the host and the environment (17, 20). Biofilm bacteria exhibit reduced sensitivity to antibiotics and cleansing agents (18, 66). Commensal strains that colonize the gastrointestinal (GI) tract as well as strains that emerge as pathogens, such as uropathogenic *E. coli* (UPEC), when they egress from the GI tract into the urinary tract commonly produce curli *in vitro* (7, 33, 44). UPEC strains command much attention in the laboratory and the clinic due to the significant prevalence of urinary tract infection (UTI) caused by UPEC in the form of acute infections as well as chronic and recurrent infections that require long-term antibiotic therapy and are often associated with life-threatening sequelae that can include antibiotic resistance and sepsis (5, 12, 28, 74). UPEC strains engage in a remarkable and well-studied genetic and molecular cascade to assemble type 1 and P pili, which are bona fide virulence factors associated with infections of the bladder and kidney, respectively (6, 22, 47, 51, 55). Yet clinical isolates differ tremendously in their phenotypes *in vitro* and *in vivo* due to the myriad of other molecular features that differentiate them and their interactions with the host (30, 54). We are interested in the contribution of functional amyloids to biofilm structure and function, particularly among UPEC strains. The coproduction of curli and cellulose enables the elaboration of bacterial biofilms formed on agar and at the air-liquid interface and attached to polyvinyl chloride (PVC) surfaces (13, 36, 68). Recent *in vivo* studies provided evidence that curli confer a fitness advantage to UPEC strains, as reflected in bladder and kidney bacterial titers in a mouse UTI model (13), and that curli and cellulose modulate the immune response (43). Curli were also identified in human patient urine samples by electron microscopy and by antibody reactivity, indicating that curli are expressed in humans (43).

The motivation behind the desire to inhibit the assembly of curli and *E. coli* biofilm formation is obvious, as biofilms are implicated in most infectious diseases and there is accumulating evidence that bacterial amyloids contribute to the environmental persistence and pathogenicity of uropathogenic and enterohem-

Received 30 November 2011 **Accepted** 20 February 2012
Published ahead of print 2 March 2012
Address correspondence to Lynette Cegelski, cegelski@stanford.edu.
Supplemental material for this article may be found at http://aem.asm.org/.

doi:10.1128/AEM.07743-11

orrhagic organisms, e.g., *E. coli* and *Salmonella* species (4, 35, 50). Toward such goals, small-molecule inhibitors have been discovered that prevent the assembly of curli-integrated biofilms of *E. coli* (13). The antimicrobial peptide LL-37 also inhibits the formation of curli (43). Other molecules prevent and disrupt the amyloid-integrated biofilms formed by the soil-dwelling organism *B. subtilis* in which the amyloid fibers are comprised of the TasA protein (46). In chemical genetic approaches, small-molecule inhibitors also provide the opportunity to serve as probes of protein assembly events if they interrupt distinct steps in the amyloid assembly cascade that are identified and examined to learn about the important protein-protein interactions en route to curli fiber assembly, for example. In the same spirit, small molecules that increase the expression or elaboration of amyloid fibers and influence the formation and architecture of biofilms also provide value in evaluations of the contributions of amyloid fibers to microbial biofilms. Moreover, as the transcriptional regulation of curli genes is complex, it is valuable to identify stimuli that upregulate protein expression to improve our understanding of how bacteria respond to their environment (75) and how amyloid fibers contribute to bacterial physiology. The influence of ethanol and other environmental and physiological stress agents, e.g., peroxide, detergents, desiccation, temperature, and nutrient limitation, has been studied extensively to elucidate the sometimes complex effects of those agents on bacterial behavior (49, 52, 62, 72). Ethanol has been shown to increase the pathogenicity of *Acinetobacter baumannii*, an opportunistic pathogen noted for its unusual ability to metabolize hydrocarbons and alcohols (10, 41).

Ethanol has also been demonstrated to upregulate biofilm production among *E. coli* and *Salmonella* species grown under various conditions by initiating a global stress response that elicits widespread changes in gene transcription profiles, including influences on cellulose production (31, 34, 82). However, biofilm formation is complex and the expression of various biofilm factors is dependent on growth conditions.

In this contribution, we describe the influence of moderate concentrations of DMSO and ethanol with respect to increases in curli production and biofilm formation by *E. coli* growing under conditions that are typically considered ideal for the expression of curli. We present the molecular profiles and phenotypes resulting from the increased elaboration of amyloid fibers and demonstrate that these changes are associated with increases in curli gene transcription. The influence of DMSO is particularly specific to curli gene upregulation and provides a valuable tool to examine contributions of curli to bacterial physiology and community behavior. We also illustrate that solid-state nuclear magnetic resonance (NMR) has the sensitivity and resolution to profile the global carbon composition of the insoluble and intact biofilms and should be of value in future efforts, as new methods are needed to analyze and quantitatively define biofilm composition and architecture. Collectively, our data support the notion that amyloid-integrated biofilm formation in *E. coli* involves a balance of curli and other extracellular matrix components, including cellulose. *E. coli* are poised to alter this balance in response to environmental stimuli. Tilting the balance by increasing amyloid content impacts community form and function.

MATERIALS AND METHODS

Agglutination assay. UTI89, UTI89Δ*csgA*, MC4100, and MC4100Δ*csgA* strains were grown in YESCA (yeast extract [0.5 g/liter], Casamino Acids [10 g/liter]) or LB broth containing various concentrations of DMSO or ethanol and at 26°C or 37°C, as indicated, with shaking at 200 rpm. The agglutination phenotype was evaluated after 24 h. Bacterial cell numbers (CFU/ml) were enumerated at the same time using the drop-plate method (39).

Western blot analysis. Cell-associated curli proteins CsgA and CsgG were examined by immunoblot assays as described previously (13). After the agglutination phenotype determination, the bacterial cultures were used for the Western blot analysis. Whole-cell samples with equivalent cell numbers were prepared as cell pellets of 1 ml of cell culture with an optical density at 600 nm (OD_{600}) of 1.0. Each pellet was treated with 100 μl of hexafluoroisopropanol (HFIP) to dissociate curli subunits (13). HFIP was removed by vacuum centrifugation, and samples were resuspended in sodium dodecyl sulfate-polyacrylamide gel electrophoresis (SDS-PAGE) loading buffer. Protein gel electrophoresis was carried out using 12% SDS-PAGE gels (Invitrogen) and blotted onto 0.2-μm-pore-size nitrocellulose transfer membranes (Whatman). The polyclonal rabbit antiserum to CsgA or CsgG was used as the primary antibody, and horseradish peroxidase (HRP)-conjugated goat anti-rabbit antibody (Pierce) was used as the secondary antibody (56).

Microarray analysis. For the preparation of each sample for microarray analysis, 12 ml of bacterial culture was mixed with 24 ml of RNAprotect bacterial reagent (Qiagen), incubated for 5 min, and centrifuged for 10 min at 5,000 × *g*. The pellet was used for total RNA extraction using an RNeasy Minikit (Qiagen). The total RNA extraction, cNDA synthesis, GeneChip hybridization, and microarray scanning were performed at SeqWright (Houston, TX). A GeneChip *E. coli* 2.0 array (Affymetrix) was used for the hybridization, and all procedures followed a standard Affymetrix protocol. The intensity of each spot in the microarray was quantified by the use of Affymetrix GeneChip operating software (GCOS) and normalized.

Biofilm assays. Colony biofilm formation was initiated by spotting 10 μl of overnight bacterial culture onto a YESCA agar plate with or without 4% DMSO (vol/vol) or 2% ethanol (vol/vol) (46). Colony morphology was observed after 48 h of growth at 26°C. In order to assess cellulose production of agar-grown cells and biofilms, 1 ml of calcofluor white (also known as Fluorescent Brightener 28) (100 μg/ml) was added to bacterial colonies growing on agar plates after 48 h of growth. Plates were visualized and photographed over a UV light table to document the fluorescence associated with cellulose-bound calcofluor. Biofilm production in YESCA broth attached to plastic (polyvinyl chloride [PVC]) was determined using the Kolter crystal violet assay as described previously (59). Briefly, bacterial cells were grown in 96-well PVC plates; unattached cells were washed away; and cells remaining associated with the PVC wells were stained with 0.1% crystal violet. The extent of biofilm formation was quantified by measuring the absorbance of crystal violet at OD_{595} after dissolving the PVC-associated biomass in 95% ethanol. The percent biofilm values represent the increases in biofilm formation in the presence of various concentrations of DMSO and ethanol relative to biofilm formation when neither compound was present. The mean data of triplicate individual experiments were used, and error bars represent the standard deviations. Pellicle formation was initiated by inoculating 4 μl of an overnight bacterial culture grown in YESCA broth into 4 ml of YESCA in 12-well-plate wells and incubation at 26°C. Pellicle formation was inspected visually and assessed by perturbation with a pipette tip after 72 h of growth.

Electron microscopy. Transmission electron microscopy (TEM) was used to image broth-grown bacteria. Bacteria were pelleted, resuspended in phosphate-buffered saline (PBS), and applied directly onto 300-mesh copper grids coated with Formvar film (Electron Microscopy Sciences [EMS], Hatfield, PA) for 2 min. The samples in grids were washed 5 times with deionized water and negatively stained with 2% uranyl acetate for 90 s. After 5 min of drying, electron microscopy was performed with a Jeol 1230 TEM. Bacterial pellicles were harvested for scanning electron microscopic analysis after 5 days of incubation without shaking at 26°C. Har-

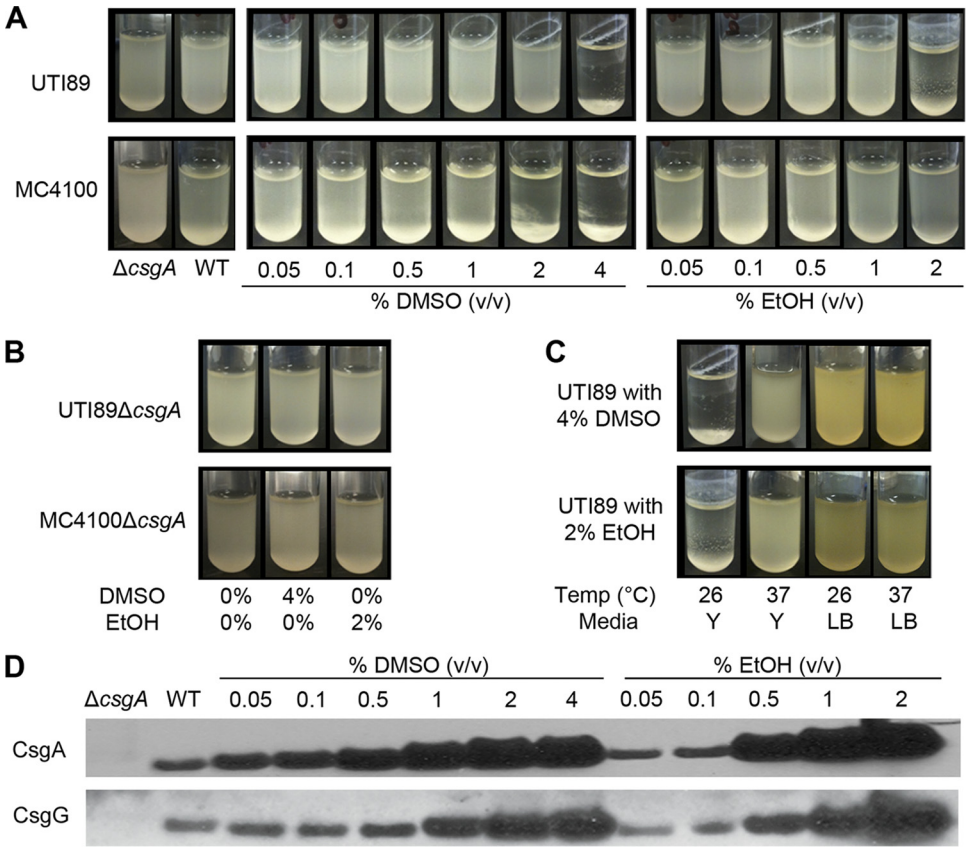

FIG 1 The chemical-associated agglutination phenotype in shaking broth. (A) Agglutination was evaluated after growth for 24 h in YESCA broth at 26°C with shaking at 200 rpm. UTI89 agglutination was observed in 4% DMSO and 2% ethanol. Agglutination of MC4100 was observed only in the presence of DMSO (2 and 4%). WT, wild type. (B) The solvent-associated agglutination phenotype was curli dependent. All samples were grown in YESCA broth at 26°C with shaking at 200 rpm. (C) Agglutination in 4% DMSO and 2% ethanol was tested as a function of temperature (26°C or 37°C) and medium (YESCA or LB broth) and was temperature and nutrient dependent. (D) CsgA and CsgG protein production levels were compared by Western blot analysis of UTI89 whole cells grown in YESCA broth for 24 h at 26°C with shaking at 200 rpm in the presence and absence of DMSO and EtOH. Y, YESCA broth, LB, LB broth; v/v, vol/vol.

vested pellicles were fixed using a solution of 2% gluteraldehyde–4% formaldehyde–0.1 M sodium cacodylate buffer (pH 7.3) overnight and then postfixed with 1% osmium tetroxide in 0.1 M sodium cacodylate buffer. Fixed pellicle samples were dehydrated in a series of increasing concentrations of ethanol (50%, 70%, 95%, and 100%), inserted into a critical point dryer (CPD) to remove residual ethanol with carbon dioxide, and then coated with gold-palladium and visualized with a Hitachi S-3400N scanning electron microscope.

Solid-state NMR spectroscopy. Samples for NMR analysis were prepared as described above and washed in 10 mM Tris buffer (pH 7.4), pelleted, frozen, and lyophilized. [$^{13}C_2$]DMSO (99% enriched) was purchased from Isotec. ^{13}C cross-polarization magic-angle spinning (CPMAS) experiments (70) were performed using a six-frequency transmission line probe with a 12-mm-long, 6-mm-inside-diameter analytical coil and a Chemagnetics/Varian magic-angle spinning ceramic stator as employed previously (14). The spectrometer was controlled by a Tecmag pulse programmer. Lyophilized samples of approximately 100 mg were packed in thin-wall 5-mm-outside-diameter zirconia rotors and were spun at 7,143 Hz. Spectra were obtained at 125.7 MHz for ^{13}C with a p-pulse length of 8 ms for carbon. Proton-carbon CPMAS transfers were made with a radiofrequency field of 62.5 kHz and a contact time of 2 ms. Proton dipolar decoupling was 100 kHz during data acquisition, and an acquisition delay of 5 s was employed. Each spectrum represents the accumulation of approximately 16,000 scans.

RESULTS

Curli-dependent agglutination in shaking broth. Small-molecule inhibitors with limited water solubility are often prepared as DMSO or ethanol stock solutions, and, although final solvent concentrations are usually less than 0.1%, solvent controls are always performed in biological assays to evaluate whether the carrier solvent alone influences measured activity. In contrast, high concentrations of DMSO and ethanol are used to impart sterility and kill microorganisms. At the low concentrations (<0.1%) typical of most whole-cell assays and as used in previous curlicide studies, DMSO and ethanol have had no obvious effect on the biogenesis of curli (13). Yet we discovered that growth of UTI89 and MC4100 with shaking in YESCA broth at higher, but still sublethal, concentrations of DMSO and ethanol resulted in an obvious agglutination phenotype in which cells replicated but aggregated and settled out of solution (Fig. 1A). This phenotype was curli dependent and was not exhibited by the UTI89Δ*csgA* or MC4100Δ*csgA* strain (Fig. 1B). MC4100 is the *E. coli* strain in which curli biogenesis was first described. The more recent studies involving the molecular determinants of curli assembly have likewise employed MC4100. MC4100 is a traditionally used laboratory K-12 strain that expresses curli but produces neither cellulose, a major *E. coli* biofilm

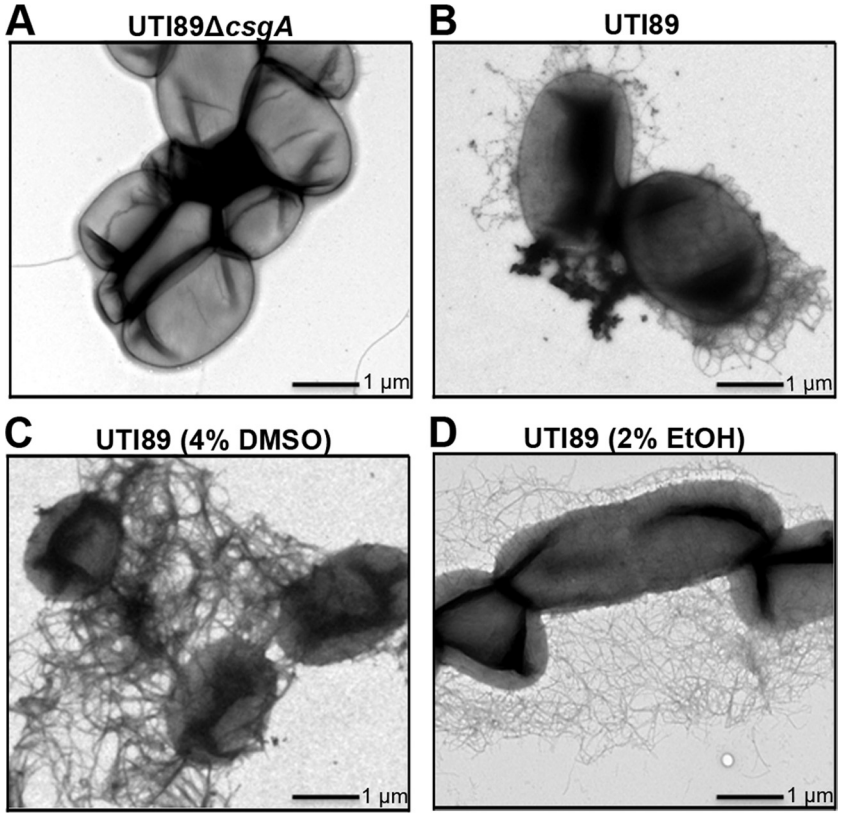

FIG 2 Evaluation of increased curli production by electron microscopy. Representative transmission electron microscopy images of UTI89 show increased curli production. UTI89Δ*csgA* (A) and UTI89 (B to D) strains were grown for 48 h with shaking in YESCA broth at 26°C in the absence (B) or presence of 4% DMSO (C) or 2% ethanol (D).

determinant, nor type 1 pili; it does not form appreciable biofilm on glass or plastic or at an air-liquid interface (61). Thus, as expected, MC4100 was not observed attached to the glass and exhibited only agglutination. UTI89 is a prototypical biofilm-competent strain that forms biofilms on agar, on plastic, and at an air-liquid interface (2, 42, 48, 79, 81). The presence of UTI89 attached to the walls of the glass culture tube near the meniscus was observed in addition to agglutination (Fig. 1A). Agglutination was not observed in YESCA broth at 37°C or in LB broth at any temperature (Fig. 1C), consistent with the preferential expression of curli genes in YESCA broth at low temperature. Measured MIC values (vol/vol) of 16% DMSO and 8% ethanol were consistent among the compared strains (MC4100, UTI89, and UTI89Δ*csgA*) grown with shaking in YESCA broth at 26 and 37°C. A minor lag in growth kinetics was observed in 2% ethanol (see Fig. S1 in the supplemental material) as determined by spectrophotometry (OD_{600}), and yet cell viability values after 16 to 24 h were consistently between 2×10^9 and 3×10^9 CFU/ml under all conditions, as shown by enumeration after dilution and plating. Cell viability in ethanol was impaired at concentrations exceeding 4% ethanol (vol/vol).

Immunoblot analyses of whole cells grown in shaking broth in the presence and absence of DMSO and ethanol were performed in order to test the hypothesis that agglutination was correlated with increased curli protein production. Curli production per cell increased markedly for UTI89 as a function of DMSO and ethanol concentration, as assessed by detection of CsgA, the major fiber subunit (Fig. 1D). In the presence of 4% DMSO, CsgA and CsgG levels were 3.9 and 3.0 times higher than in untreated cells, respectively, as determined by densitometry. In the presence of 2% ethanol, CsgA and CsgG levels increased by factors of 6.1 and 5.0, respectively. The increase for MC4100 was more modest, with each of the proteins exhibiting an increase in band intensity of 35% (see Fig. S2 in the supplemental material). Increased levels of CsgG were also detected, and Ponceau S staining of the membranes confirmed proper sample preparation and lane loading, with samples normalized by equivalent cell numbers (see Fig. S3 in the supplemental material). To determine whether other clinical isolates associated with uropathogenesis were affected by DMSO, we assayed a panel of other well-characterized UPEC isolates and found that 10/18 behaved similarly to UTI89 with respect to CsgA production (see Fig. S4 in the supplemental material). Four strains did not produce detectable curli under these growth conditions. The remaining four strains produced curli, but the influence of solvent was slight and increases in band intensity were not greater than 25%.

The major interest in examining functional amyloid formation, particularly among *E. coli* strains, relates to the contribution of amyloids to community behavior and biofilm formation. Thus, for the subsequent experiments reported here, which concerned gene regulation and the functional implications of enhanced curli production in biofilms, we focused our study on the biofilm-competent and prototypical UPEC strain UTI89. Increased curli production by UTI89 was confirmed visually in the transmission electron micrographs obtained for the UTI89 samples described above that were prepared by shaking in YESCA broth in the presence of 4% DMSO or 2% ethanol (Fig. 2).

Solvent-induced changes in gene transcription. Microarray analysis was performed on the samples grown in shaking broth after 24 h in order to determine whether the increase in curli production was driven at the transcriptional level and to broadly profile gene expression to determine if the response was a general one that influenced many pathways in the cell, such as is commonly ascribed to ethanol stress and tolerance, or if the effect was more specific to curli production. The entire microarray data set is available (see Table S1 in the supplemental material). The most dramatic effect observed for cells treated with DMSO and with ethanol was the marked upregulation of the *csgB* and *csgA* genes (Table 1). In the presence of DMSO, *csgB* was upregulated 13-fold and *csgA* 12-fold. In the presence of ethanol, *csgB* and *csgA* were upregulated 14-fold and 8-fold, respectively. In addition, the microarray measurements of the same cells grown for 24 h revealed only a modest increase (under 2-fold) in the transcription of the *csgD* regulator gene and of the *csgE*, *csgF*, and *csgG* genes that encode their respective curli assembly proteins (Table 1). A summary of results for all genes whose transcription changed by more than 2-fold in the case of DMSO and 3-fold in the case of ethanol is provided in Tables S2 and S3 in the supplemental material. Treatment with ethanol was associated with anticipated changes to many additional genes that are appreciated to be involved in the complex physiology of ethanol stress and tolerance (9, 40, 53). Yet even for ethanol-treated cells, *csgB* and *csgA* are the two genes whose transcription was identified as being the most highly altered in the microarray.

We restricted our further consideration of gene regulation to the DMSO-treated samples that exhibited a more curli-selective response. Notably, *csgD* gene transcription was not influenced significantly in DMSO-treated samples at 24 h (upregulated 1.6-fold). Other genes that would be expected to change in response to a significant increase in *csgD* expression were also unaltered: e.g., *bcsA-bcsC*, responsible for cellulose synthesis (65, 84); *yhiU*, encoding O antigen (32); and the *rpoS* regulon and its expressed stationary-phase sigma factor σ^s, a subunit of RNA polymerase that acts as a master regulator of the general stress response in *E. coli* (37, 49) (Table 1). Thus, the DMSO-induced upregulation of curli production appeared to exhibit specificity for the *csgBA* operon. The transcriptional changes associated with several key genes (*csgA*, *csgB*, *csgD*, *csgE*, *csgF*, *csgG*, *rpoS*, and *cpxP*) after growth for 24 h were confirmed by quantitative real-time PCR (qRT-PCR) (see Fig. S5 in the supplemental material). In addition, transcription of these genes was assessed at an earlier time point, after 4 h of growth, in the presence or absence of added solvent (see Fig. S5 in the supplemental material). Using qRT-PCR and the established primers listed in Table S4 in the supplemental material, an increase in transcription of *csgA* and *csgB* was already observed at 4 h, and transcription was further upregulated at 24 h (to levels equivalent to those reported in the microarray results), whereas *csgD* exhibited a higher fold increase (1.8) in expression at 4 h but exhibited no significant increase at 24 h. *rpoS* changes were unremarkable and exhibited a slight decrease after 24 h (see Fig. S5 in the supplemental material).

Enhanced colony morphology and biofilm formation. The production of both curli and cellulose results in the formation of a complex extracellular matrix that promotes biofilm formation (68). Indeed, these two molecular features contribute to the hallmark colony morphology exhibited by *E. coli* and also *Salmonella* species, as presented for UTI89 in Fig. 3A. As expected, the curli mutant, i.e., the UTI89Δ*csgA* strain, did not exhibit this phenotype (Fig. 3A); neither did MC4100, which does not produce cellulose (see Fig. S2 in the supplemental material). In the presence of either 4% DMSO or 2% ethanol, UTI89 colonies grew larger in diameter (35% larger in DMSO and 55% larger in ethanol) but exhibited wrinkling that was less pronounced. These changes were curli dependent; no significant changes in colony size or morphology were observed for the UTI89Δ*csgA* strain (Fig. 3A).

In addition to the exhibition of the typical curli- and-cellulose-dependent colony morphology on agar, UTI89 forms curli-dependent biofilms in YESCA broth attached to plastic (PVC) and at the air-liquid interface, also referred to as pellicles (13). We tested whether DMSO and ethanol would influence curli-integrated biofilm formation in these two biofilm models. In the presence of 4% DMSO, biofilm formation increased by more than 100% as determined by crystal violet staining, dissolution, and quantification (Fig. 3B). However, ethanol did not cause an appreciable increase in biofilm formation attached to PVC, a process during which the bacteria grow under static conditions. This is consistent with our not having observed an increase in the extent of attachment to glass culture tubes under shaking conditions (Fig. 1). The extent of pellicle formation was visualized macroscopically. More-robust pellicles were formed in the presence of DMSO and ethanol, as emphasized by exerting pressure on the growing film with a plastic pipette tip (Fig. 3C). The UTI89Δ*csgA* strain did not form pellicles even in the presence of DMSO and ethanol (data not shown). Scanning electron microscopy was employed to examine in more detail the physical changes in pellicle structure induced by DMSO and ethanol. The micrographs of pellicles grown in medium supplemented with DMSO or ethanol displayed an increased elaboration of curli fibers, particularly in the DMSO-grown pellicle, and an increased extent of connections among cells compared with pellicles formed in untreated medium (Fig. 4).

Whole-cell NMR comparison of carbon pools among UTI89 pellicles. It was obvious from the protein profiles obtained by immunoblotting and the electron micrographs that curli production was increased in response to DMSO and ethanol. Bacteria have been described as metabolizing unusual molecules found in the environment under various conditions (69). In order to assess whether the dramatic DMSO-mediated enhancements in curli production, colony morphology, and biofilm formation could be attributed in part to direct metabolism or catabolism of DMSO as a carbon source, we employed ^{13}C CPMAS solid-state NMR spectroscopy (70) on intact pellicles formed by strain UTI89 in the presence of DMSO or [$^{13}C_2$]DMSO.

Inspection of the NMR spectra (Fig. 5) permitted a simple compositional comparison of the total carbon pools of the DMSO-treated pellicles. Notably, the spectrum acquired of pellicles formed in the presence of [$^{13}C_2$]DMSO was comparable to that of an unlabeled sample. The only notable increase appears at 39 ppm and corresponds to the isotropic chemical shift of DMSO methyl carbons and can be attributed to residual [$^{13}C_2$]DMSO associated with or resident in the cells but not to DMSO that was transformed into alternate carbon-containing metabolites that would exhibit a different chemical shift. Thus, as anticipated, DMSO treatment results in the upregulation of curli production but the DMSO is not itself utilized directly as a carbon source to contribute to the increased production of extracellular matrix material and biomass.

TABLE 1 Comparison of curli- and biofilm-associated gene expression levels for UTI89 grown in the presence of 4% DMSO or 2% EtOH as determined by microarray analysis[a]

Protein category	Gene (s)	Description	Fold change	
			DMSO[b]	EtOH[c]
Curli	*csgA*	Curli major subunit	13.3	8.4
	csgB	Curli minor subunit	12.5	14.1
	csgD	Curli regulator	1.6	1.1
	csgE	Curli assembly	1.4	−1.2[c]
	csgF	Curli assembly	1.7	1.1
	csgG	Curli assembly/transport	1.5	1.0
Fimbria/flagellum	*fimB*, *fimD*	Type 1 fimbria regulator, export/assembly	1.2	−1.5
	fliO	Flagellar biosynthesis protein	−1.3	−1.3
	flhE	Flagellar protein	−1.1	−1.4
Cellulose	*bcsA*	Cellulose synthase	1.1	−1.2
Stress	*gadA*	Glutamate decarboxylase isozyme	1.7	3.8
	gadB	Glutamate decarboxylase isozyme	1.5	4.4
	gadC	Acid sensitivity protein, putative transporter	1.5	2.1
	gadE	DNA-binding transcriptional activator	−1.2	6.6
	hdeA	Acid resistance protein	1.2	2.8
	hdeB	Acid resistance protein	1.1	4.5
	cspA	Major cold shock protein	−1.3	2.0
	cspC	Cold shock-like protein	2.3	3.5
	yfiA	Ribosome-associated cold shock protein	2.2	1.3
Biofilm	*rpoD*	RNA polymerase, sigma 70 (sigma D) factor	1.1	2.6
	rpoS	RNA polymerase, sigma S (sigma 38) factor	1.1	2.4
	rpoE	RNA polymerase, sigma 24 (sigma E) factor	1.0	3.2
	bssR	Biofilm formation regulatory protein	2.1	−2.3
	arcA	Two-component response regulator	1.4	3.4
Colanic acid	*wcaB*	Colanic acid biosynthesis	1.2	−1.6
	wcaM	Colanic acid biosynthesis protein	−1.4	−3.3
	wzxC	Colanic acid exporter	1.6	−3.9
sRNA	*omrA*	Small RNA	1.3	−2.7
	ryjA	Small RNA	1.6	−2.6
	gcvB	Small RNA	1.2	−2.3
	ryeD	Small RNA	−1.4	−2.1
	sokC	Small RNA	1.4	−2.1
	rprA	Small RNA	1.1	2.8
	psrD	Small RNA	−1.1	3.5
	ryeA	Small RNA	1.0	3.7
	glmZ	Small RNA	−1.6	5.0
	hfq	RNA-binding protein Hfq	1.6	2.8
Ribosomal proteins[d]	*rps*	30S rRNAs	−1.1[e]	3.8[f]
	rpl	50S rRNAs	−0.9[g]	4.1[h]

[a] Bacterial cells were grown in YESCA broth for 24 h at 26°C.
[b] Data represent fold changes associated with growth in broth plus 4% DMSO relative to growth in untreated broth.
[c] Data represent fold changes associated with growth in broth plus 2% EtOH relative to growth in untreated broth.
[d] Numerical ribosomal protein data represent averages of 23 30S rRNA genes and 34 50S rRNA genes.
[e] Fold-change values ranged from −1.6 to 1.0.
[f] Fold-change values ranged from 2.1 to 5.5.
[g] Fold-change values ranged from −1.5 to 1.1.
[h] Fold-change values ranged from −1.1 to 5.6.

DISCUSSION

Bacteria continually sense and respond to their environment. They communicate with one another via small-molecule signals through quorum sensing that permits density-dependent gene regulation and coordination of community activities such as swarming and biofilm formation (19, 29, 73, 76). Microbial responses to environmental signals can be complex and are often context dependent (75). Bacteria may respond differently to their environment depending on the nature of the growth conditions and their metabolic state. This is particularly evident in studies of

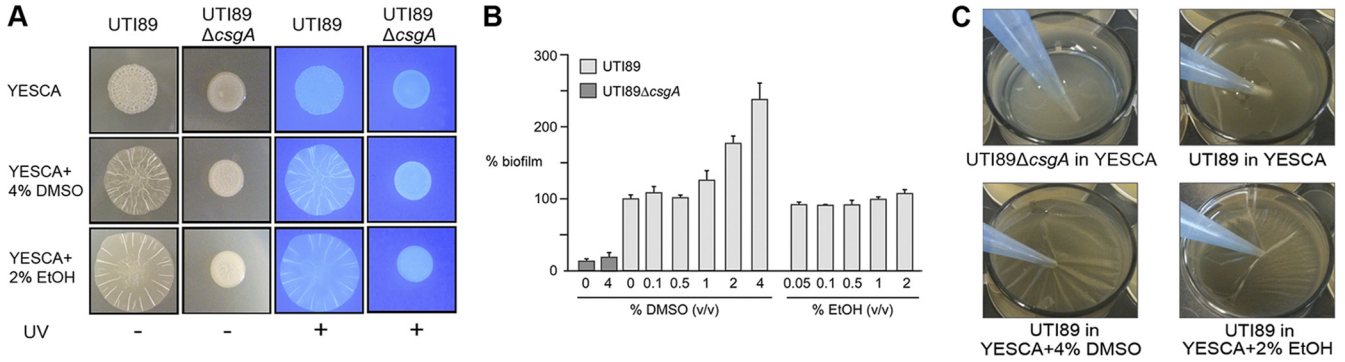

FIG 3 Chemical influence on biofilm formation. (A) The colony morphology of UTI89 and UTI89Δ*csgA* strains was documented after a 48-h growth period on YESCA agar in the absence (top row) or presence of 4% DMSO (middle row) or 2% ethanol (bottom row). Calcofluor was added to bacteria after growth on YESCA agar plates (left panels), and photographs of plates observed during back-lit excitation on a UV light table were obtained (right panels). (B) DMSO increased formation of biofilms attached to plastic. Bacteria were grown at 26°C for 48 h in PVC 96-well microplates containing YESCA broth. Plastic-associated biomass was stained with 0.1% crystal violet, washed, and quantified by OD_{595} determination after crystal violet dissolution in ethanol. Biofilm formation in the presence of added solvent was compared to UTI89 growth in YESCA broth (designated 100%). Error bars represent the standard deviations of the comparative values of percent biofilm from biofilm assays performed in triplicate. (C) DMSO and ethanol enhanced pellicle formation. Photographs were taken after 72 h of incubation at 26°C in static YESCA broth in 12-well plates.

adhesion and biofilm formation. Multiple adhesive systems have been studied for their functional roles in environmental persistence and host pathogenesis. The expression of these systems may vary as a function of time and place, and the systems may have redundant roles. Thus, for the study of individual features and virulence factors, conditions must be identified under which the influence of each factor can be examined and the factors can manipulated with interpretable outcomes. Formation of UPEC biofilms attached to plastic is dependent on the presence of curli and independent of the presence of type 1 pili when biofilms are grown in YESCA medium, which is ideal for curli expression, but is independent of the presence of curli and dependent on the presence of type 1 pili when biofilms are grown in LB medium (13). Furthermore, pellicle formation by strain UTI89 is curli dependent and is observed only in YESCA medium (13). The recent elucidation of these conditions and the requirement of curli for UPEC biofilm formation at the air-liquid interface permit the selective study of contributions of curli to UTI89 community behavior.

We demonstrated here that curli gene transcription and protein expression increased dramatically in response to DMSO and ethanol. Many thorough and well-examined transcriptional analyses of biofilm formation, though powerful in their comparisons and conclusions, were not focused on curli. Some were performed under conditions characterized by very low curli expression levels, e.g., in human urine (26, 71), or under conditions in which curli expression and protein levels were not examined (53). The latter study, in particular, examined the complex response of *E. coli* to ethanol (53). Thus, our microarray data are of general value to

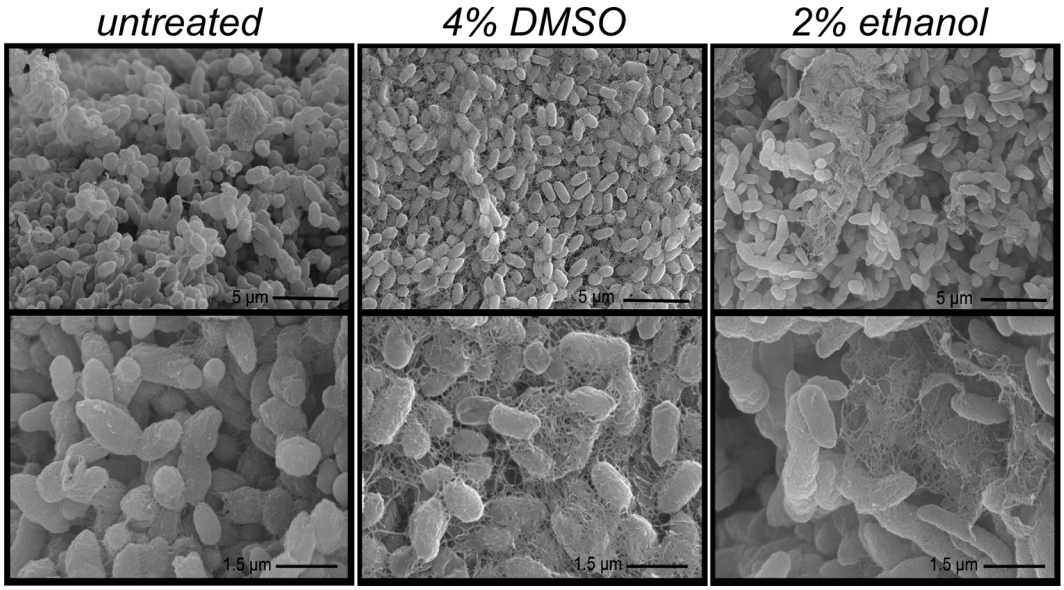

FIG 4 Visualization of pellicles by scanning electron microscopy. Bacterial pellicles of UTI89 were examined after 5 days of incubation at 26°C in static YESCA broth and visualized at ×5,000 (top panels) and ×15,000 (lower panels) magnification. Left column, pellicle grown in YESCA broth; middle column, pellicle grown in YESCA broth containing 4% DMSO; right column, pellicle grown in YESCA broth containing 2% ethanol.

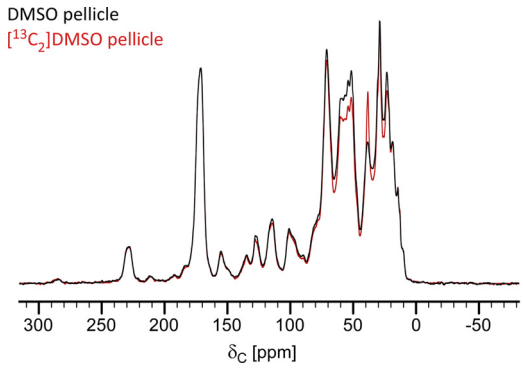

FIG 5 Comparative analysis of carbon pools in intact pellicles by solid-state NMR spectroscopy. The natural-abundance ^{13}C CPMAS NMR spectra provided a complete accounting of the carbon contributions in intact pellicles formed by UTI89 in the presence of DMSO. Except for the enhancement in peak intensity at 39 ppm (the isotropic carbon chemical shift of DMSO), growth in medium supplemented with labeled [$^{13}C_2$]DMSO did not result in other carbon peak intensity increases.

studies of curli and curli-integrated biofilms, as they were performed on curli-expressing *E. coli* grown at 26°C in YESCA medium, conditions used for curli expression in many curli biogenesis and functional studies. The importance of this is also illustrated in Fig. 1, as no remarkable influence on community behavior was observed during growth under alternative medium or temperature conditions. Although unanticipated, the selective upregulation of *csgA* and *csgB* gene expression was the most remarkable gene transcription response to each solvent identified by microarray analysis. The microarray data for DMSO-treated bacteria, which were more straightforward to consider, as growth in DMSO did not activate the global stress pathways associated with ethanol stress and tolerance (36, 37, 53), revealed no obvious influence on other genes canonically ascribed to curli or to biofilm regulation as described above. More-rigorous temporal studies may reveal time-dependent transcriptional changes that occurred earlier than those we examined. Alternatively, a new mechanism to upregulate *csgA* and *csgB* transcription or to stabilize the mRNA may underlie this phenomenon. The future dissection of the detailed mechanism of this genetic response may contribute to our understanding of the complex regulatory network that influences curli biogenesis and biofilm formation and may also lead to the identification of new strategies to inhibit curli gene expression.

From the microbial and structural ecology standpoint, there is tremendous interest in relating the molecular contributions of bacterial biofilms to function and, ultimately, in mapping biofilm architectures at the atomic level. The ability of DMSO to increase curli production presented a valuable opportunity to assess the functional consequences of extracellular amyloid fibers on *E. coli* community behavior and allowed the tuning of amyloid production among samples by the use of the same strain and under the same growth conditions. Our results revealed that tuning the production of curli altered functions ascribed to bacterial communities, including cellular agglutination and biofilm formation. Yet it is currently not understood at the molecular and atomic level how amyloid fibers contribute to biofilm architectures or how they interact with other biofilm components, such as cellulose.

Solid-state NMR spectroscopy can provide a noninvasive comparative assessment of carbon pools in intact amyloid-integrated biofilms. We determined directly from the spectra of pellicle bacteria formed in the presence of [$^{13}C_2$]DMSO that DMSO was not being metabolized or transformed by *E. coli.* The consideration of the possible unusual metabolism of DMSO was noted in a previous study of common microorganisms (excluding methylotrophs, known for their ability to metabolize DMSO) that were tolerant of 100% DMSO (25), yet this notion was not tested. This NMR approach is a general one that can address such questions of metabolism and transformation of metabolites under other circumstances, particularly when exogenously added components are used. Looking to the future, it should be possible to perform further measurements involving biosynthetic isotopic labeling and NMR-detection schemes to define in detail the specific contributions to biofilm spectra.

Although such interpretations are speculative, the possible benefit to *E. coli* of upregulating curli production in response to exogenous DMSO and ethanol may be gleaned from the electron micrographs and the influence of increased curli production on the nature of pellicle formation at the air-liquid interface. Curli are hydrophobic proteins, and, like the chaplins of Gram-positive bacteria (16, 23) and TasA amyloid fibers in *B. subtilis* (64), curli enable enhanced colonization of bacteria at the air-liquid interface. At the interface, the extracellular hydrophobic proteins would have an increased tendency to associate away from water and promote pellicle growth and stability. Furthermore, ethanol may be encountered in certain host niches, such as in the gastrointestinal tract and in the bladder, and may be relevant in pathogenesis. The gastrointestinal environment harbors *E. coli* strains, such as UTI89, that can become uropathogenic when they egress from the intestinal niche and enter the urogenital tract, although we know very little currently about the mechanisms that promote ascension in the urinary tract compared with the abundance of molecular, genetic, and immunological cross-talk that takes place once *E. coli* colonizes the bladder.

Overall, the recruitment of small molecules to influence the expression of curli emphasizes the significant functional implications of amyloid production by *E. coli. E. coli* can respond to environmental stimuli, including DMSO and ethanol, to tilt the compositional balance of the extracellular matrix by increasing amyloid production to alter community structure and strengthen cohesion. These data support our developing model of the extracellular matrix as an organized assembly of polymeric components, including amyloid fibers, in which composition relates to bacterial physiology and community function.

ACKNOWLEDGMENTS

We thank Jacob Schaefer for NMR spectrometer access and Scott Hultgren for the gift of curli antibodies. We thank Swaine L. Chen for valuable discussion.

L.C. holds a Career Award at the Scientific Interface from the Burroughs Wellcome Fund. J.M.M. is the recipient of a predoctoral NSF fellowship. L.C. gratefully acknowledges support from the NIH Director's New Innovator Award Program (DP2OD007488), Stanford University, and a Stanford Terman fellowship.

REFERENCES

1. **Alteri CJ, et al.** 2007. Mycobacterium tuberculosis produces pili during human infection. Proc. Natl. Acad. Sci. U. S. A. **104**:5145–5150.
2. **Anderson GG, et al.** 2003. Intracellular bacterial biofilm-like pods in urinary tract infections. Science **301**:105–107.
3. **Barak JD, Gorski L, Naraghi-Arani P, Charkowski AO.** 2005. Salmonella

enterica virulence genes are required for bacterial attachment to plant tissue. Appl. Environ. Microbiol. **71**:5685–5691.
4. **Barnhart MM, Chapman MR.** 2006. Curli biogenesis and function. Annu. Rev. Microbiol. **60**:131–147.
5. **Blango MG, Mulvey MA.** 2010. Persistence of uropathogenic Escherichia coli in the face of multiple antibiotics. Antimicrob. Agents Chemother. **54**:1855–1863.
6. **Bock K, et al.** 1985. Specificity of binding of a strain of uropathogenic Escherichia coli to Gal alpha 1–4Gal-containing glycosphingolipids. J. Biol. Chem. **260**:8545–8551.
7. **Bokranz W, Wang XD, Tschape H, Romling U.** 2005. Expression of cellulose and curli fimbriae by Escherichia coli isolated from the gastrointestinal tract. J. Med. Microbiol. **54**:1171–1182.
8. **Boyer RR, et al.** 2007. Influence of curli expression by Escherichia coli O157:H7 on the cell's overall hydrophobicity, charge, and ability to attach to lettuce. J. Food Prot. **70**:1339–1345.
9. **Brynildsen MP, Liao JC.** 2009. An integrated network approach identifies the isobutanol response network of Escherichia coli. Mol. Syst. Biol. **5**:277.
10. **Camarena L, Bruno V, Euskirchen G, Poggio S, Snyder M.** 2010. Molecular mechanisms of ethanol-induced pathogenesis revealed by RNA-sequencing. PLoS Pathog. **6**:e1000834.
11. **Capstick DS, Jomaa A, Hanke C, Ortega J, Elliot MA.** 2011. Dual amyloid domains promote differential functioning of the chaplin proteins during Streptomyces aerial morphogenesis. Proc. Natl. Acad. Sci. U. S. A. **108**:9821–9826.
12. **Cegelski L, Marshall GR, Eldridge GR, Hultgren SJ.** 2008. The biology and future prospects of antivirulence therapies. Nat. Rev. Microbiol. **6**:17–27.
13. **Cegelski L, et al.** 2009. Small-molecule inhibitors target Escherichia coli amyloid biogenesis and biofilm formation. Nat. Chem. Biol. **5**:913–919.
14. **Cegelski L, Schaefer J.** 2006. NMR determination of photorespiration in intact leaves using in vivo 13CO2 labeling. J. Magn. Reson. **178**:1–10.
15. **Chapman MR, et al.** 2002. Role of Escherichia coli curli operons in directing amyloid fiber formation. Science **295**:851–855.
16. **Claessen D, et al.** 2003. A novel class of secreted hydrophobic proteins is involved in aerial hyphae formation in Streptomyces coelicolor by forming amyloid-like fibrils. Genes Dev. **17**:1714–1726.
17. **Costerton JW, et al.** 1987. Bacterial biofilms in nature and disease. Annu. Rev. Microbiol. **41**:435–464.
18. **Costerton JW, Lewandowski Z, Caldwell DE, Korber DR, Lappin-Scott HM.** 1995. Microbial biofilms. Annu. Rev. Microbiol. **49**:711–745.
19. **Daniels R, Vanderleyden J, Michiels J.** 2004. Quorum sensing and swarming migration in bacteria. FEMS Microbiol. Rev. **28**:261–289.
20. **Donlan RM, Costerton JW.** 2002. Biofilms: survival mechanisms of clinically relevant microorganisms. Clin. Microbiol. Rev. **15**:167–193.
21. **Dueholm MS, et al.** 2010. Functional amyloid in Pseudomonas. Mol. Microbiol. **77**:1009–1020.
22. **Eden CS, Leffler H.** 1980. Glycosphingolipids of human urinary tract epithelial cells as possible receptors for adhering Escherichia coli bacteria. Scand. J. Infect. Dis. Suppl. **1980**:(Suppl. 24):144–147.
23. **Elliot MA, et al.** 2003. The chaplins: a family of hydrophobic cell-surface proteins involved in aerial mycelium formation in Streptomyces coelicolor. Genes Dev. **17**:1727–1740.
24. **Epstein EA, Chapman MR.** 2008. Polymerizing the fibre between bacteria and host cells: the biogenesis of functional amyloid fibres. Cell. Microbiol. **10**:1413–1420.
25. **Fedorka-Cray PJ, Cray WC, Jr, Anderson GA, Nickerson KW.** 1988. Bacterial tolerance of 100% dimethyl sulfoxide. Can. J. Microbiol. **34**: 688–689.
26. **Ferrières L, Hancock V, Klemm P.** 2007. Specific selection for virulent urinary tract infectious Escherichia coli strains during catheter-associated biofilm formation. FEMS Immunol. Med. Microbiol. **51**:212–219.
27. **Fowler DM, Koulov AV, Balch WE, Kelly JW.** 2007. Functional amyloid—from bacteria to humans. Trends Biochem. Sci. **32**:217–224.
28. **Foxman B.** 2003. Epidemiology of urinary tract infections: incidence, morbidity, and economic costs. Dis. Mon. **49**:53–70.
29. **Fuqua C, Greenberg EP.** 2002. Listening in on bacteria: acyl-homoserine lactone signalling. Nat. Rev. Mol. Cell Biol. **3**:685–695.
30. **Garofalo CK, et al.** 2007. Escherichia coli from urine of female patients with urinary tract infections is competent for intracellular bacterial community formation. Infect. Immun. **75**:52–60.
31. **Gerstel U, Romling U.** 2001. Oxygen tension and nutrient starvation are major signals that regulate agfD promoter activity and expression of the multicellular morphotype in Salmonella typhimurium. Environ. Microbiol. **3**:638–648.
32. **Gibson DL, et al.** 2006. Salmonella produces an O-antigen capsule regulated by AgfD and important for environmental persistence. J. Bacteriol. **188**:7722–7730.
33. **Goller CC, Seed PC.** Revisiting the Escherichia coli polysaccharide capsule as a virulence factor during urinary tract infection. Virulence **1**:333–337.
34. **Goodarzi H, et al.** 2010. Regulatory and metabolic rewiring during laboratory evolution of ethanol tolerance in E. coli. Mol. Syst. Biol. **6**:378.
35. **Gophna U, et al.** 2001. Curli fibers mediate internalization of Escherichia coli by eukaryotic cells. Infect. Immun. **69**:2659–2665.
36. **Gualdi L, et al.** 2008. Cellulose modulates biofilm formation by counteracting curli-mediated colonization of solid surfaces in Escherichia coli. Microbiology **154**:2017–2024.
37. **Gualdi L, Tagliabue L, Landini P.** 2007. Biofilm formation-gene expression relay system in Escherichia coli: modulation of σ^S-dependent gene expression by the CsgD regulatory protein via σ^S protein stabilization. J. Bacteriol. **189**:8034–8043.
38. **Hammar M, Bian Z, Normark S.** 1996. Nucleator-dependent intercellular assembly of adhesive curli organelles in Escherichia coli. Proc. Natl. Acad. Sci. U. S. A. **93**:6562–6566.
39. **Hoben HJ, Somasegaran P.** 1982. Comparison of the pour, spread, and drop plate methods for enumeration of Rhizobium spp. in inoculants made from presterilized peat. Appl. Environ. Microbiol. **44**:1246–1247.
40. **Ingram LO.** 1990. Ethanol tolerance in bacteria. Crit. Rev. Biotechnol. **9**:305–319.
41. **Juni E.** 1978. Genetics and physiology of Acinetobacter. Annu. Rev. Microbiol. **32**:349–371.
42. **Justice SS, et al.** 2004. Differentiation and developmental pathways of uropathogenic Escherichia coli in urinary tract pathogenesis. Proc. Natl. Acad. Sci. U. S. A. **101**:1333.
43. **Kai-Larsen Y, et al.** 2010. Uropathogenic Escherichia coli modulates immune responses and its curli fimbriae interact with the antimicrobial peptide LL-37. PLoS Pathog. **6**:e1001010.
44. **Kanamaru S, et al.** 2006. Increased biofilm formation in Escherichia coli isolated from acute prostatitis. Int. J. Antimicrob. Agents **28**:21–25.
45. **Kikuchi T, Mizunoe Y, Takade A, Naito S, Yoshida S.** 2005. Curli fibers are required for development of biofilm architecture in Escherichia coli K-12 and enhance bacterial adherence to human uroepithelial cells. Microbiol. Immunol. **49**:875–884.
46. **Kolodkin-Gal I, et al.** 2010. D-Amino acids trigger biofilm disassembly. Science **328**:627–629.
47. **Kuehn MJ, Heuser J, Normark S, Hultgren SJ.** 1992. P pili in uropathogenic E. coli are composite fibres with distinct fibrillar adhesive tips. Nature **356**:252–255.
48. **Kulesus RR, Diaz-Perez K, Slechta ES, Eto DS, Mulvey MA.** 2008. Impact of the RNA chaperone Hfq on the fitness and virulence potential of uropathogenic Escherichia coli. Infect. Immun. **76**:3019–3026.
49. **Landini P.** 2009. Cross-talk mechanisms in biofilm formation and responses to environmental and physiological stress in Escherichia coli. Res. Microbiol. **160**:259–266.
50. **Larsen P, et al.** 2007. Amyloid adhesins are abundant in natural biofilms. Environ. Microbiol. **9**:3077–3090.
51. **Martinez JJ, Mulvey MA, Schilling JD, Pinkner JS, Hultgren SJ.** 2000. Type 1 pilus-mediated bacterial invasion of bladder epithelial cells. EMBO J. **19**:2803–2812.
52. **Matin A.** 1992. Genetics of bacterial stress response and its applications. Ann. N. Y. Acad. Sci. **665**:1–15.
53. **Moen B, et al.** 2009. Global responses of Escherichia coli to adverse conditions determined by microarrays and FT-IR spectroscopy. Can. J. Microbiol. **55**:714–728.
54. **Mulvey MA.** 2002. Adhesion and entry of uropathogenic Escherichia coli. Cell. Microbiol. **4**:257–271.
55. **Mulvey MA, et al.** 1998. Induction and evasion of host defenses by type 1-piliated uropathogenic Escherichia coli. Science **282**:1494–1497.
56. **Nenninger AA, et al.** 2011. CsgE is a curli secretion specificity factor that prevents amyloid fibre aggregation. Mol. Microbiol. **81**:486–499.
57. **Nenninger AA, Robinson LS, Hultgren SJ.** 2009. Localized and efficient curli nucleation requires the chaperone-like amyloid assembly protein CsgF. Proc. Natl. Acad. Sci. U. S. A. **106**:900–905.
58. **Olsen A, Jonsson A, Normark S.** 1989. Fibronectin binding mediated by

a novel class of surface organelles on Escherichia coli. Nature **338**:652–655.
59. **O'Toole GA, Kolter R.** 1998. Initiation of biofilm formation in Pseudomonas fluorescens WCS365 proceeds via multiple, convergent signalling pathways: a genetic analysis. Mol. Microbiol. **28**:449–461.
60. **Pawar DM, Rossman ML, Chen J.** 2005. Role of curli fimbriae in mediating the cells of enterohaemorrhagic Escherichia coli to attach to abiotic surfaces. J. Appl. Microbiol. **99**:418–425.
61. **Peters JE, Thate TE, Craig NL.** 2003. Definition of the Escherichia coli MC4100 genome by use of a DNA array. J. Bacteriol. **185**:2017–2021.
62. **Rasouly A, Ron EZ.** 2009. Interplay between the heat shock response and translation in Escherichia coli. Res. Microbiol. **160**:288–296.
63. **Robinson LS, Ashman EM, Hultgren SJ, Chapman MR.** 2006. Secretion of curli fibre subunits is mediated by the outer membrane-localized CsgG protein. Mol. Microbiol. **59**:870–881.
64. **Romero D, Aguilar C, Losick R, Kolter R.** 2010. Amyloid fibers provide structural integrity to Bacillus subtilis biofilms. Proc. Natl. Acad. Sci. U. S. A. **107**:2230–2234.
65. **Römling U, Rohde M, Olsen A, Normark S, Reinkoster J.** 2000. AgfD, the checkpoint of multicellular and aggregative behaviour in Salmonella typhimurium regulates at least two independent pathways. Mol. Microbiol. **36**:10–23.
66. **Ryu JH, Beuchat LR.** 2005. Biofilm formation by Escherichia coli O157:H7 on stainless steel: effect of exopolysaccharide and curli production on its resistance to chlorine. Appl. Environ. Microbiol. **71**:247–254.
67. **Ryu JH, Kim H, Beuchat LR.** 2004. Attachment and biofilm formation by Escherichia coli O157:H7 on stainless steel as influenced by exopolysaccharide production, nutrient availability, and temperature. J. Food Prot. **67**:2123–2131.
68. **Saldaña Z, et al.** 2009. Synergistic role of curli and cellulose in cell adherence and biofilm formation of attaching and effacing Escherichia coli and identification of Fis as a negative regulator of curli. Environ. Microbiol. **11**:992–1006.
69. **Sasikala C, Ramana CV.** 1998. Biodegradation and metabolism of unusual carbon compounds by anoxygenic phototrophic bacteria. Adv. Microb. Physiol. **39**:339–377.
70. **Schaefer J, Stejskal EO.** 1976. C-13 nuclear magnetic-resonance of polymers spinning at magic angle. J. Am. Chem. Soc. **98**:1031–1032.
71. **Schembri MA, Kjærgaard K, Klemm P.** 2003. Global gene expression in Escherichia coli biofilms. Mol. Microbiol. **48**:253–267.
72. **Shenhar Y, Rasouly A, Biran D, Ron EZ.** 2009. Adaptation of Escherichia coli to elevated temperatures involves a change in stability of heat shock gene transcripts. Environ. Microbiol. **11**:2989–2997.
73. **Shrout JD, et al.** 2006. The impact of quorum sensing and swarming motility on Pseudomonas aeruginosa biofilm formation is nutritionally conditional. Mol. Microbiol. **62**:1264–1277.
74. **Soto S, et al.** 2007. Biofilm formation in uropathogenic Escherichia coli strains: relationship with prostatitis, urovirulence factors and antimicrobial resistance. J. Urol. **177**:365–368.
75. **Stanley NR, Lazazzera BA.** 2004. Environmental signals and regulatory pathways that influence biofilm formation. Mol. Microbiol. **52**:917–924.
76. **Stock AM, Robinson VL, Goudreau PN.** 2000. Two-component signal transduction. Annu. Rev. Biochem. **69**:183–215.
77. **Uhlich GA, Cooke PH, Solomon EB.** 2006. Analyses of the red-dry-rough phenotype of an Escherichia coli O157:H7 strain and its role in biofilm formation and resistance to antibacterial agents. Appl. Environ. Microbiol. **72**:2564–2572.
78. **Uhlich GA, Gunther NW, IV, Bayles DO, Mosier DA.** 2009. The CsgA and Lpp proteins of an Escherichia coli O157:H7 strain affect HEp-2 cell invasion, motility, and biofilm formation. Infect. Immun. **77**:1543–1552.
79. **Ulett GC, Mabbett AN, Fung KC, Webb RI, Schembri MA.** 2007. The role of F9 fimbriae of uropathogenic Escherichia coli in biofilm formation. Microbiology **153**:2321.
80. **Vidal O, et al.** 1998. Isolation of an Escherichia coli K-12 mutant strain able to form biofilms on inert surfaces: involvement of a new ompR allele that increases curli expression. J. Bacteriol. **180**:2442–2449.
81. **Wright KJ, Seed PC, Hultgren SJ.** 2007. Development of intracellular bacterial communities of uropathogenic Escherichia coli depends on type 1 pili. Cell. Microbiol. **9**:2230–2241.
82. **Yoo BK, Chen J.** 2009. Influence of culture conditions and medium composition on the production of cellulose by Shiga toxin-producing Escherichia coli cells. Appl. Environ. Microbiol. **75**:4630–4632.
83. **Zogaj X, Bokranz W, Nimtz M, Romling U.** 2003. Production of cellulose and curli fimbriae by members of the family Enterobacteriaceae isolated from the human gastrointestinal tract. Infect. Immun. **71**:4151–4158.
84. **Zogaj X, Nimtz M, Rohde M, Bokranz W, Romling U.** 2001. The multicellular morphotypes of Salmonella typhimurium and Escherichia coli produce cellulose as the second component of the extracellular matrix. Mol. Microbiol. **39**:1452–1463.